JOURNAL OF AGRICULTURAL AND FOOD CHEMISTRY

Detection and Identification of Bacteria in an Isolated System with Near-Infrared Spectroscopy and Multivariate Analysis

DIMITRIS ALEXANDRAKIS,*,†,§ GERARD DOWNEY,† AND AMALIA G. M. SCANNELL§

Teagasc, Ashtown Food Research Centre, Ashtown, Dublin 15, Ireland, and College of Life Sciences, School of Agriculture, Food Science and Veterinary Medicine, Agriculture and Food Science Centre, University College Dublin, Belfield, Dublin 4, Ireland

Near-infrared (NIR) transflectance spectra of *Listeria innocua* FH, *Lactococcus lactis*, *Pseudomonas fluorescens*, *Pseudomonas mendocina*, and *Pseudomonas putida* suspensions were collected and investigated for their potential use in the identification and classification of bacteria. Unmodified spectral data were transformed (first and second derivative) using the Savitzsky−Golay algorithm. Principal component analysis (PCA), partial least-squares discriminant analysis (PLS2-DA), and soft independent modeling of class analogy (SIMCA) were used in the analysis. Using either full cross-validation or separate calibration and prediction data sets, PLS2 regression classified the five bacterial suspensions with 100% accuracy at species level. At *Pseudomonas* genus level, PLS2 regression classified the three *Pseudomonas* species with 100% accuracy. In the case of SIMCA, prediction of an unknown sample set produced correct classification rates of 100% except for *L. innocua* FH (77%). At genus level, SIMCA produced correct classification rates of 96.7, 100, and 100% for *P. fluorescens*, *P. mendocina*, and *P. putida*, respectively. This successful investigation suggests that NIR spectroscopy can become a useful, rapid, and noninvasive tool for bacterial identification.

KEYWORDS: Bacteria; near-infrared; NIR; multivariate analysis; prediction; spectroscopy

INTRODUCTION

Near-infrared (NIR) spectroscopy (750–2500 nm) has become a very popular technique for a wide range of analyses in various industries (*1*–*8*). The utility of this technique arises mainly from its ability to perform fast, accurate, nondestructive, and simultaneous measurements of chemical components in complex sample matrices. Additionally, it can provide information about structural and physical properties of biological materials. Information present in near-infrared spectra originates in overtone and combination vibrations of molecular groupings such as O−H, N−H, C−H, and S−H bonds. Absorption bands arising from these vibrations are typically very broad, leading to spectra that often lack detailed structure and in which it can be difficult to assign individual features to specific chemical components. On the other hand, the spectra do contain significant amounts of information that is obscured by the overlapping nature of the specific absorption bands present. Improvements in instrumentation and the increasing availability of chemometric software (*9*–*11*) have contributed significantly to the tremendous expansion of this technique. Multivariate (multiple wavelength) data analysis tools and calibration techniques (e.g., principal component analysis or partial least-squares regression) are often employed to extract the desired chemical information from any given spectral data set.

Bacterial identification and differentiation by mid-infrared spectroscopy (2500−5000 nm) has been investigated since the middle of the last century (*12*–*16*), but shortcomings in available instrumentation led to the discontinuation of these studies for several decades. The development of modern mid-infrared spectroscopy (early 1970s), Fourier transform techniques, and chemometrics together with advances in computer technology gave a new impulse to this research field. In 1991, Naumann et al. (*17*) reported that Fourier-transformed mid-infrared (FT-IR) absorption spectra of microorganisms were highly specific, fingerprint-like patterns that could be used for identification purposes. The simplicity and versatility of Fourier transform infrared spectroscopy make it a versatile technique for the rapid differentiation, classification, identification, and large-scale screening of microbes at the subspecies level. The potential of FT-IR to detect spoilage in chicken has been investigated (*18*), and results obtained suggest that accurate estimates of bacterial loads can be calculated from measurements taken from the meat surface. It is proposed by the authors that proteolysis is the main indicator for the onset of spoilage when microorganisms have

* Author to whom correspondence should be addressed (telephone +35318059946; Fax +35318059550; e-mail dimitris.alexandrakis@teagasc.ie).
† Teagasc.
§ University College Dublin.

10.1021/jf073407x CCC: $40.75
Published on Web 04/24/2008

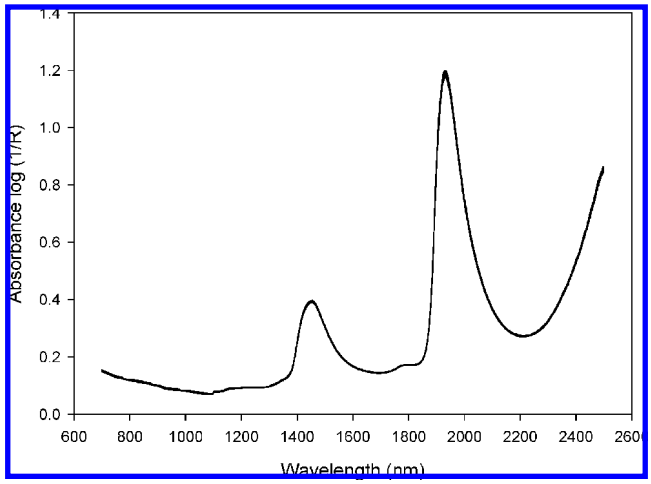

Figure 1. Unmodified absorbance spectra of all bacterial suspensions.

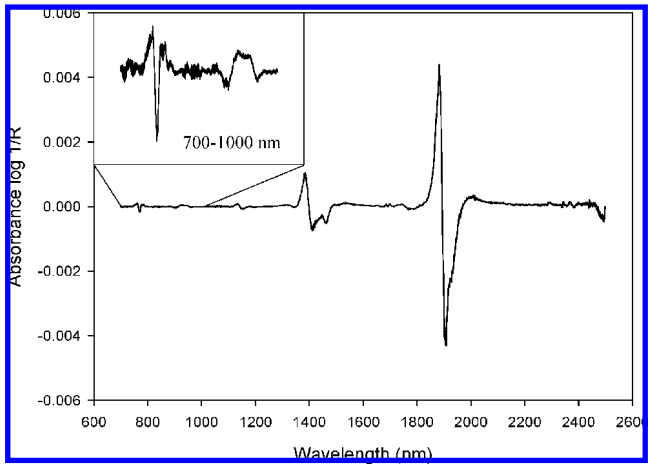

Figure 2. Second-derivative spectra of bacterial suspensions (gap size = 5 data points, two to the left and two to the right of the data point transformed). The 700–1000 nm range has been enlarged for visual purposes.

reached a concentration of 10^7 cfu g^{-1}. Al-Qadiri et al. (*19*) used FT-IR spectroscopy and multivariate analysis to detect *Pseudomonas aeruginosa* and *Escherichia coli* inoculated into bottled drinking water. Anodisc membrane filters were used to isolate the bacteria, and the spectra acquired had sufficient information to allow detection of pure cultures with the aid of multivariate analysis.

More recently, the potential of NIR and multivariate techniques to identify microbial species has been investigated. FT-NIR measurements in conjunction with such multivariate techniques such as principal component analysis (PCA) and soft independent modeling of class analogy (SIMCA) of transformed spectra in the region 5100−4400 cm^{-1} (1960−2272 nm) enabled discrimination between certain bacterial species (*E. coli* spp., *Pseudomonas* spp., *Bacillus* spp., *Listeria innocua*) (*20*). Dubois et al. demonstrated that the use of near-infrared chemical imaging cards operating in the spectral region of 1200–2350 nm possesses the specificity required to differentiate bacteria on the basis of their NIR spectra (*21*). Lin et al. (*22*) reported that visible and short-wave NIR spectral data combined with PCA were capable of detecting changes in microbial loads in chicken muscle once the total aerobic plate count (APC) increased slightly above one log cycle; accurate ($R = 0.91$, SEP = 0.48 log cfu g^{-1}) quantification of bacterial loads in chicken muscle was achieved by these authors using a PLS-based method. In fact, after 8 h, the APC was determined to be $\log_{10}$ (APC) = 5.67. These data correlated well with additional work done by Rodriguez-Saona et al. (*23*). Finally, Suthiluk et al. (*24*) reported that prediction of bacterial contamination in shredded cabbage was possible using near-infrared spectroscopy in the short-wavelength region (700–1100 nm).

The long-term objectives of the work reported here were to evaluate the feasibility of applying NIR spectroscopy and multivariate data analysis to microbial identification in vivo and thereby develop a rapid, nondestructive method to identify microbes on food. This paper is the first in a planned series that attempts to identify bacterial species suspended individually in saline solution and in a mixture of species suspended in saline solution and to repeat that work on food systems. In this initial study, efforts focused on investigating the potential of NIR to identify and enumerate *Lactococcus lactis*, *Listeria innocua*, *Pseudomonas fluorescens*, *Pseudomonas putida*, *Pseudomonas mendocina* suspended in a saline solution.

MATERIALS AND METHODS

Growth Conditions and Sample Preparation. The following bacterial cultures were obtained from the University College Dublin (UCD) microbiological culture collection: *L. lactis* 3417, *L. innocua* FH 2333, *P. fluorescens* 2088, *P. putida* 49128, and *P. mendocina* (isolated from a beef carcass and identified using 16S DNA sequencing). All bacteria were cultivated aerobically on tryptic soy agar (TSA; CM0131, Oxoid, Basingstoke, U.K.). From each plate, an isolated single colony was aseptically collected with a sterile loop and suspended in 10 mL of brain heart infusion broth (BHIl CM225, Oxoid). The bacteria were grown at 37 °C for 24 ± 2 h, and 1 mL of each bacterial suspension was aseptically transferred to 10 mL of maximum recovery diluent (MRD; CM0733, Oxoid). This suspension was centrifuged (4000 rpm for 10 min at 4 °C) and washed twice in MRD, yielding a concentrated (approximately 7.4 × 10^7 cfu/mL) working solution. This working solution was then serially diluted (dilution factors 10^{-1}, 10^{-2}, 10^{-3}, 10^{-4}, 10^{-5}, and 10^{-6}) in MRD and kept at 8 °C for no longer than 10 min prior to NIR measurements to minimize growth. Samples were then allowed to equilibrate to room temperature (20 ± 3 °C) for about 10 min, and NIR measurements were taken. A total of 418 samples were analyzed (90 each of *L. lactis* 3417, *L. innocua* FH 2333, and *P. fluorescens* 2088, 71 of *P. mendocina*, and 77 of *P. putida*).

Near-Infrared Spectroscopy. Visible and near-infrared transflectance spectra (400–2498 nm) were recorded on a NIRSystems 6500 scanning monochromator (FOSS NIRSystems, Silver Spring, MD) fitted with a sample transport module. Samples (0.1 mL) were placed in a camlock cell fitted with a gold-plated backing plate (0.1 mm sample thickness; part IH-0355-1). The backing plate is constructed with flanges around its rim to produce the exact sample thickness specified; gaps in this flange permit the egress of excess sample to the rear of the plate during cell closure. Instrument control and initial spectral manipulation were performed with WinISI II software (v1.04a; Infrasoft International, Port Matilda, MD). Between samples, the sample cell components were washed with ethanol (70% v/v) and rinsed with sterilized MRD solution. Cells were dried using paper tissue. Bacterial suspensions were scanned in duplicate with the camlock cell being rotated through 180° between scans to minimize any possible effect due to settling. The mean of these duplicate spectra was used in all subsequent calculations. Given that the samples were in aqueous solution and fine temperature control was not possible, the order of sample scanning was randomized with respect to species, concentration, and day of scanning.

Chemometrics. Spectral (log 1/*R*) files were exported from WinISI in NSAS format and then imported into The Unscrambler (v 9.2; CAMO A/S, Oslo, Norway) for data analysis. Samples were randomized and divided into two groups: a calibration group that consists of two-thirds of the samples and a prediction group that consists of the remaining one-third. Sample assignment to each group was performed by selecting every third sample as a member of the prediction group; remaining samples were assigned to the calibration group. Random selection did not generate equal size groups,

necessitating minor manual adjustments to ensure that all dilution factors, within each bacterial species, were well represented in both the calibration and prediction sample sets. Preliminary analysis of the calibration data set for unusual or outlying samples was performed by PCA. SIMCA was used for predicting class membership. In this work, five principal component models to describe each bacterial species were developed using the calibration samples. Models were developed for various wavelength ranges and using raw, first-derivative, and second-derivative spectra. These five models were then deployed simultaneously to classify the prediction sample set.

Partial least-squares discriminant analysis (PLS2-DA) was used to develop models to discriminate between bacterial species. PLS2-DA is a version of PLS in which several *Y*-variables are modeled simultaneously, thus taking advantage of possible correlations or colinearity between *Y*-variables. The discriminant analysis approach assumes that a sample has to be a member of one of the classes included in the analysis. Each class is represented by an indicator variable, that is, a binary variable with a value of 1 for members of that class and 0 for nonmembers. By building a PLS2 model with indicator variables as *Y*, it is possible to directly predict class membership from the *X*-variables describing any given sample. Model output is a predicted value for an unknown sample; in this case, correct predictions ideally have a *Y* value of 1 for the bacterial species being predicted and 0 for the other species. In practice, values of ≥ 0.5 are interpreted as indicating membership of the group being modeled with results ≤ 0.5 indicating nonmembership. All predicted values are accompanied by a deviation that is an estimate of how reliable the prediction is. Whereas data covering the visible and the entire NIR wavelength region (400–2500 nm) were collected, models were developed and validated using this complete range and a number of subsets of that range. The most accurate models were developed using the wavelength range 700−900 nm, and only these models will be discussed in this paper. Spectral (log 1/*R*) data were analyzed without modification and after the calculation of first and second derivatives; these were calculated using the Savitzky−Golay method (*25*) and involved a number of gap sizes as detailed below. All calibrations were developed using full cross-validation.

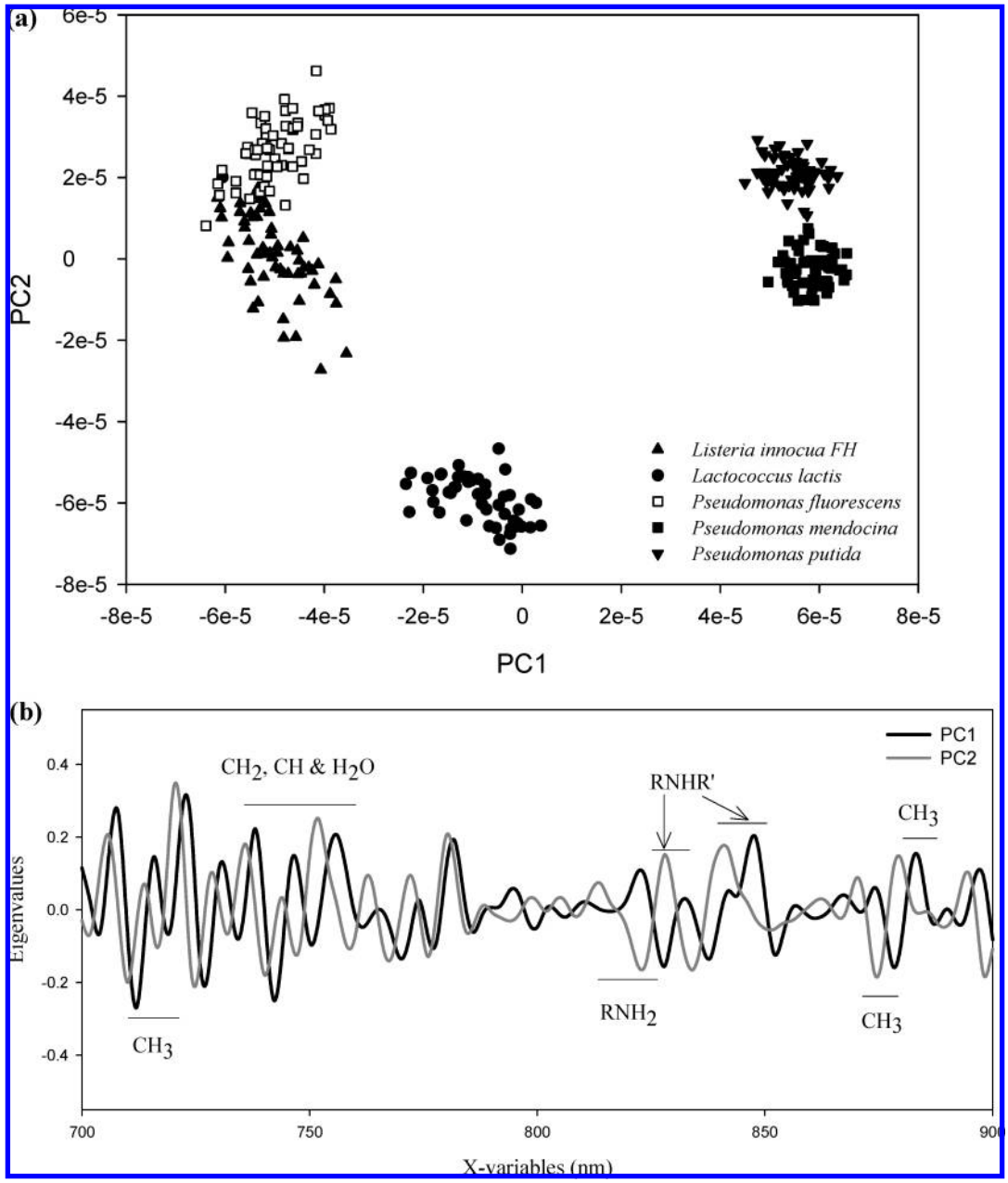

Figure 3. (**a**) PCA of second-derivative transformed spectral data over the wavelength range 700–900 nm. (**b**) Eigenvalues for PC1 and PC2 for second-derivative transformed spectral data over the wavelength range 700–900 nm.

RESULTS AND DISCUSSION

Spectra. The near-infrared spectra of all bacterial suspensions scanned are shown in **Figure 1**. These unmodified spectra show almost identical patterns for all bacterial samples with strong absorption bands around 1440 (O−H first overtone) and 1950 nm (O−H combination bands), which dominate the spectra. Bands at these wavelengths correspond to the strongest water absorption bands in the NIR region (absorption coefficients of 26 and 114 L mol^{-1} cm^{-1}, respectively) (*26*). To the naked eye, no discrimination between any of the bacterial species present is possible. Spectral derivatization, especially second derivatives, has the benefit of removing baseline sloping effects and resolving overlapping absorption bands; second-derivative spectra are shown in **Figure 2**. Features around 1440 nm have now been resolved and show some additional structure but, not surprisingly, absorption by water continues to be the main feature.

PCA. PCA of the whole data set revealed that the best separation, as judged by eye, between all of the bacterial species was found using second-derivative transformed data in the wavelength range 700−900 nm (**Figure 3a**). There were no unusual or outlying samples detected, and all were therefore used in subsequent chemometric analysis. **Figure 3a** reveals that each bacterial species formed a well-defined cluster; *P.s mendocina* and *P. putida* clustered closely together and separately from all of the other species on the right-hand side, and there was no visually detectable overlap between these two clusters. *L. lactis* bacteria formed a discrete group in the lower, central area of this figure, well-separated from all of the other species. *L. innocua* FH clustered very close to *P. fluorescens* in this two-dimensional representation, and some overlap of these two species is apparent in **Figure 3a**. Principal component 1 separates *P. mendocina* and *P. putida* from the rest of the organisms; principal component 2 separates *L. lactis* from the other organisms. Models developed using visible or wavelength range 400–900 nm were inferior to models developed using the wavelength range 700–900 nm. Consequently, the contribution of the visible range seems to be insignificant. The major outcome of this preliminary data analysis step is that the bacterial organisms studied form discrete and largely separate clusters. This strongly suggests that differentiation between the different species may be possible on the basis of their near-infrared spectra. Given that the scanning order of the bacterial suspension samples was fully randomized, this observed differentiation is highly unlikely to be an artifact resulting from sample temperature variations. **Figure 3b** is a graphical representation of principal components 1 and 2; the highest eigenvalues are found at 712, 742, 756, 828, 834, 848, 878, 882, and 898nm. This region (700–900 nm) is dominated by the absorption (third overtone) of hydrogen-bearing groups (−CH−, −OH−, and −NH−). In particular, 712 nm corresponds to $–CH_3$ absorption, 742 and 756 nm to CH_2, CH, and H_2O absorption, 828 nm to –RNHR′ and $–RNH_2$, 834 and 848 nm to RNHR′, and finally 878, 882, and 898 nm to CH_3 absorption bands (*27*). Absorbance at these wavelengths may correspond to the lipids that are largely present in bacterial cell walls but are also present in all structural elements of the cell. Due to the abundance of these substances in all living cells and the variety of possible combinations of different acyl arms and head groups, lipids can be highly species specific (*28*). Many studies have employed the use of lipid fingerprints for the taxonomic classification of bacteria (*29, 30*).

PCA was also performed to investigate the potential of NIR to detect different concentration levels within each organism for enumeration purposes. The whole data set for each bacterial species was used individually, and the category variable was the dilution factor. Unfortunately, PCA did not show any clear clustering among the six different dilution factors. When the score plots were studied carefully, it was evident that dilution factor 6 was represented in the top right-hand corner of the score plot and dilution factor 1 in the bottom left-hand corner. The rest of the dilution factors, though, were spread evenly along the whole plot, thus not allowing us to continue modeling as the degree of error and the uncertainty would be too large to proceed any further. One explanation for the separation of dilution factor 1 and dilution factor 6 would be the fact that dilution factor 6 (∼74 cfu/mL) would not contain enough structural information compared to a very concentrated dilution factor 1, resulting in the separation of the two in the score plots. On the other hand, a PCA model of dilution factor 6 for all bacterial species did separate the bacteria in clusters. The clusters were not as tight as in higher concentration dilutions, but the separation was present. For this reason all dilution factors were used in the effort to discriminate between bacterial species. This also explains why the clusters in **Figure 3a** and subsequent figures are slightly dispersed. It is due to the presence of a large concentration range within each bacterial data set.

PLS-DA. Six PLS loadings were judged to be optimal for the PLS2-DA model developed using the calibration sample set and second-derivative transformed spectral data in the wavelength range 700–900 nm. Score plots associated with this model showed clear clustering of the different bacterial organisms. The score plot on loadings 1 and 2 clustered the bacterial species in a similar manner to the score plot on components 1 and 2 for data in this spectral range (**Figure 3a**). Although most of the bacterial species were separated, *L. innocua* and *P. fluorescens* clustered very closely together; examination of a rotated 3-D score plot using higher order loadings revealed increased separation between *L. innocua* and *P. fluorescens* (**Figure 4**). The output of the PLS2-DA model is a series of regressions of each bacterial organism against all of the others; a graphical display of one such regression (separation of *L. lactis* from the rest) produced using this model is shown in **Figure 5**; this is a plot of predicted *Y* value for all prediction samples. The prediction value is shown as a circular point. The vertical lines around the point indicate the deviation, that is, whether the prediction is reliable or not. All other bacterial organisms showed similar separation from the other species. Correct predictions have a *Y* value of ≥ 0.5 for the bacterial species being predicted and ≤ 0.5 for the other species. Evaluation of the accuracy of these PLS2 models is made on the basis of errors in identification and fall into one of two classes. False-negative identifications refer to samples actually belonging to a class that are not classified as such by the class model. False-positive identifications relate to samples that do not belong to a given class but are incorrectly identified as so belonging by the relevant class model. All class models showed 100% correct classification of class members (no false negatives); no false-positive classifications were generated by the models for *P. fluorescens*, *P. mendocina*, *L. innocua*, and *L. lactis*. The *P. putida* model generated a single false-positive result, a single *P. mendocina* sample being incorrectly predicted as *P. putida* (**Table 1**). Deviations for the prediction samples are all very similar, as shown by the magnitude of the error bars associated with each sample.

SIMCA Classification. The highest correct classification results for SIMCA were achieved using a second-derivative transformation of spectral data; a summary of model performance is shown in **Table 2**. Models for *P. fluorescens*, *P.*

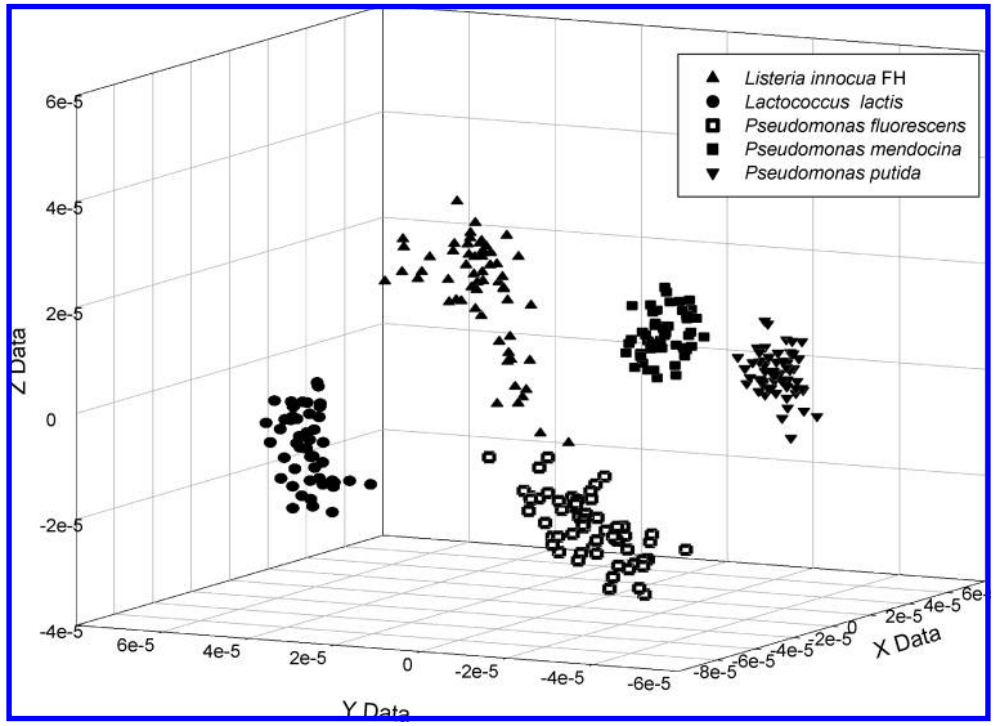

Figure 4. 3-D representation of PLS2-DA model of second-derivative transformed spectral data in the wavelength range 700–900 nm (loading 1 vs loading 2 vs loading 3).

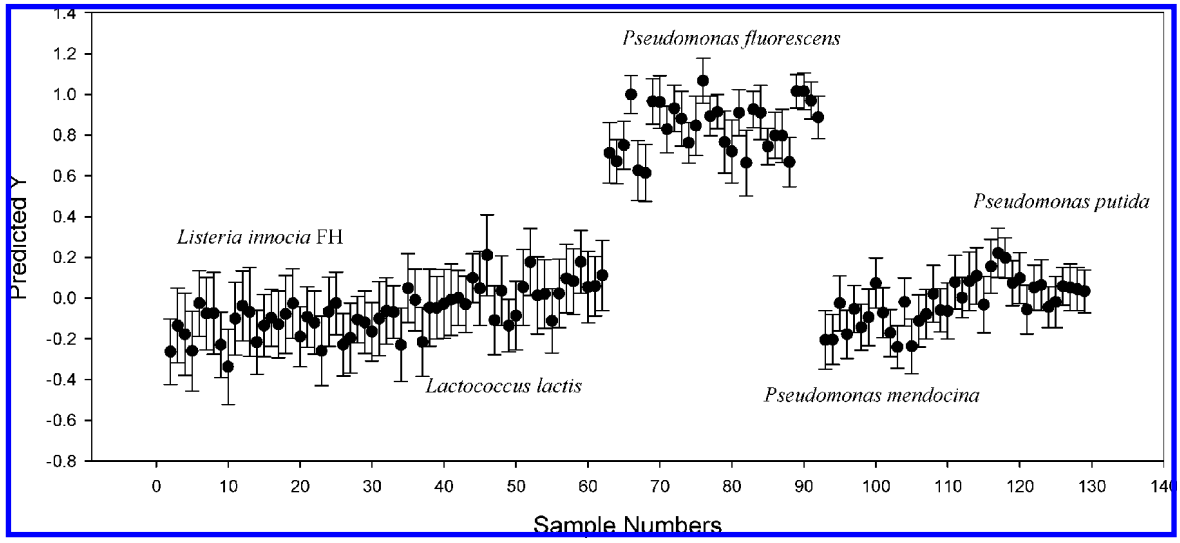

Figure 5. Prediction results for *Pseudomonas fluorescens* (PLS2-DA model, 700–900 nm wavelength range, and second-derivative transformed data).

Table 1. PLS2-DA Prediction Results (Second Derivative, 700–900 nm)

bacterium	samples correctly predicted	%	false negatives	false positives
Listeria innocua	30	100.0	0	0
Lactococcus lactis	30	100.0	0	0
Pseudomonas fluorescens	30	100.0	0	0
Pseudomonas mendocina	19	100.0	0	0
Pseudomonas putida	18	100.0	0	1 (*Ps. mend.*)

Table 2. SIMCA Classification Results (Second Derivative, 700–900 nm)

bacterium	samples correctly classified	%	false negatives	false positives
Listeria innocua	24	77.4	7	0
Lactococcus lactis	30	100.0	0	0
Pseudomonas fluorescens	30	100.0	0	22
Pseudomonas mendocina	19	100.0	0	4
Pseudomonas putida	18	100.0	0	0

mendocina, *P. putida*, and *L. lactis* produced 100% correct classification rates; in the case of *L. innocua* FH, the failure to correctly classify 7 of 24 samples produced a correct classification rate of only 77.4%. Models for *L. innocua* FH, *L. lactis*, and *P. putida* did not produce any false-positive errors, but those for *P. mendocina* and *P. fluorescens* did produce 4 and 22 false-positive misclassifications, respectively. These misclassified samples belonged to *P. putida* (*P. mendocina* model) and *L. innocua* FH (*P. fluorescens* model), respectively.

Repetition of this classification study using all of the bacterial samples or different randomly selected samples in the calibration

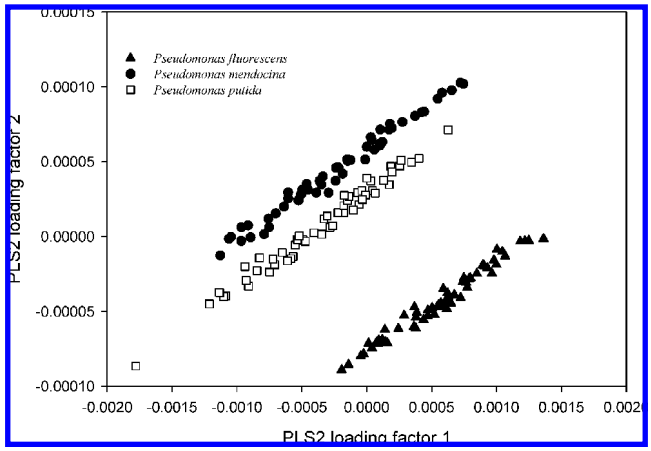

Figure 6. PLS-DA score plot of second-derivative transformed data over the wavelength range 700–1100 nm.

and validation sample sets did not change the overall pattern of SIMCA results. The main variation was a reduction in the number of false-positive classifications when all samples were used to create and validate a SIMCA model. This suggests that the use of a greater number of samples of each bacterial species and a smaller concentration range within each organism may improve the accuracy and robustness of the SIMCA models developed.

Chemometric Analysis of *Pseudomonas* Data. In the study described above, discrimination between and classification of bacterial species have been described. However, it may be that this amalgamation of levels of differentiation prevents the development of optimal models for separation of species that belong to the same genus. For this reason, the spectral data collected for the three *Pseudomonas* species was reanalyzed separately to study how well chemometric analysis of NIR spectral data could discriminate between them alone.

PLS-DA. Several wavelength ranges were investigated, but the best discriminant model (using 10 PLS factors) was created by Savitzky−Golay second-derivative transformed data over the wavelength range 700–1100 nm. A discriminant scores plot (**Figure 6**) reveals the clear separation between the bacterial strains, although *P. mendocina* and *P. putida* are quite close in this two-dimensional representation. Calibration performance on the validation sample set produced a 100% correct classification rate for all models; no false-positive identifications were made by any model. Graphical display of *P. fluorescens* results is shown in **Figure 7**. *P. putida* and *P. mendocina* have similar graphical displays.

Table 3. SIMCA Classification Results (Second Derivative, 700–1100 nm)

bacterium	samples correctly classified	%	false negatives	false positives
Pseudomonas fluorescens	29	96.7	0	0
Pseudomonas mendocina	19	100.0	0	0
Pseudomonas putida	17	81.5	4	21

SIMCA Classification. A principal component model to describe each bacterial species was developed using the calibration sample sets and a number of wavelength ranges; best results were again achieved using spectral data between 700 and 1100 nm (**Table 3**). Each model was generated using five principal components. *P. fluorescens* revealed a correct classification rate of 96.7%, whereas *P. mendocina* and *P. putida* achieved correct classification rates of 100%. A feature of these models, however, was the presence of some false-negative and false-positive identifications; in the case of *P. fluorescens*, a low figure of 2.3% of samples were wrongly identified as belonging to none (false negative) of the three strains, whereas 81.5% of *P. putida* were wrongly identified as *P. mendocina* (false positive).

The objectives of this study were to evaluate the feasibility of applying NIR spectroscopy to microbial identification and enumeration in an isolated system and subsequently develop a rapid nondestructive method to identify microbes isolated from food systems. Analysis of spectral data has revealed very promising results for discrimination and classification of unknown samples. The highest prediction and classification accuracies were achieved using second-derivative transformed spectral data in the wavelength ranges 700–900 nm. Using a confidence level of <1%, 100% correct prediction was achieved at strain level (*P. fluorescens*, *P. mendocina*, and *P. putida*); in addition, almost 100% correct prediction was achieved at species level. SIMCA classification successfully discriminated between bacteria but with a large number of false positives. Further work to improve the sensitivity of the models is required.

In comparison to previous studies in this field, apart from the fact that a different set of bacterial species was studied, the spectra obtained and investigated cover the whole near-infrared region (700–2495 nm); previously published work did not include information below 1000 nm. Therefore, the models

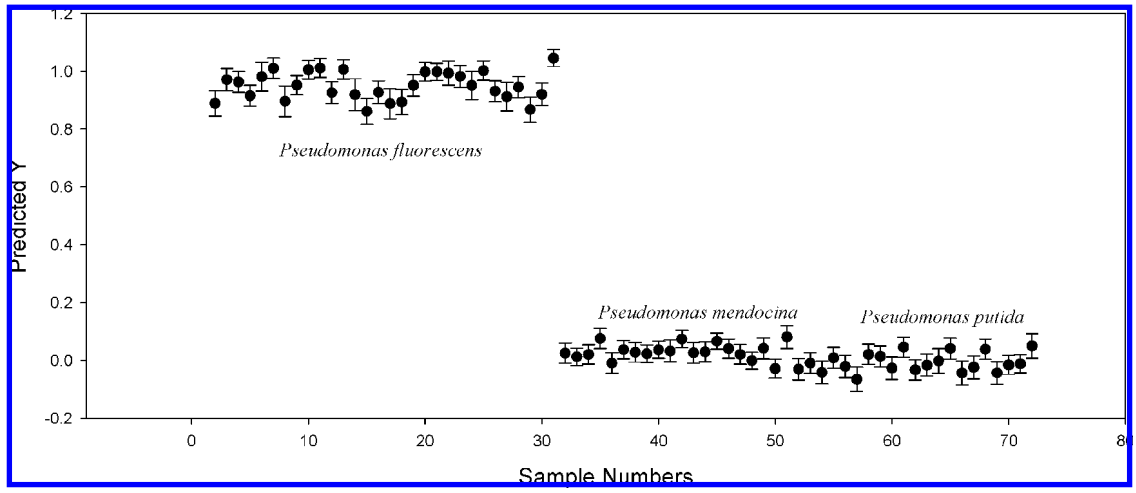

Figure 7. Prediction results for *Pseudomonas fluorescens* (PLS2-DA model, 700–1100 nm wavelength range, and second-derivative transformed data).

created in this study (700–900 nm) were able to avoid the strong water absorption bands. This finding correlates very well with near-infrared studies investigating the potential to detect microbial contamination (*22, 24*), in wihch the same spectral region was used to detect the changes in microbial loads in food systems. In addition, by obtaining transflectance spectra of liquid samples using a 0.1 mL cell with a gold background the impact of water absorption was further reduced which allowed in vivo bacterial detection and differentiation compared to previous studies in which bacterial films were used to eliminate the effect of water.

To conclude, the use of NIR spectroscopy and chemometrics shows great potential for the identification and classification of bacterial species. Further experimental work needs to be carried out so that this successful technique can be tested on a food system and thereby develop a methodology that utilizes the advantages of using NIR to detect and differentiate bacteria.

LITERATURE CITED

(1) Watson, C. A. Near infrared reflectance spectrophotometric analysis of agricultural products. *Anal. Chem.* **1977**, *49*, 835A–840A

(2) Osborne, B. G.; Fearn, T.; Hindle, P. H. *Practical NIR Spectroscopy with Applications in Food and Beverage Analysis*; Longman Scientific and Technical: Harlow, U.K., 1993.

(3) Kirsch, J. D.; Drennen, J. K. Near-infrared spectroscopy: applications in the analysis of tablets and solid pharmaceutical dosage forms. *Appl. Spectrosc. Rev.* **1995**, *30* (3), 139–174.

(4) Weyer, L. G. Near-infrared spectroscopy of organic substances. *Appl. Spectrosc. Rev.* **1985**, *21* (1/2), 1–43.

(5) Siesler, H. W. Near infrared spectroscopy of polymers. *Macromol. Chem. Macromol. Symp.* **1991**, *52*, 113–129.

(6) Kradjel, C. In *Handbook of Near-Infrared Analysis*; Burns, D. A., Ciurczak, E. W., Eds.; Dekker: New York, 2001; pp 659–701.

(7) Bunding-Lee, K. A. A comparison of mid-IR with NIR in polymer analysis. *Appl. Spectrosc. Rev.* **1993**, *28* (3), 231–284.

(8) Descales, B.; Cermelli, I.; Llinas, J. R.; Margail, G.; Martens, A. On line analysis on petrochemical units by near infrared spectrophotometry. *Analusis Mag.* **1993**, *21* (9), M25–M28.

(9) Martens, H.; Naes, T. In *Multivariate Calibration*; Wiley: Chichester, U.K., 1989.

(10) Mark, H. In *Handbook of Near-Infrared Analysis*; Burns, D. A., Ciurczak, E. W., Eds.; Dekker: New York, 2001; pp 129−184.

(11) Bjorsvik H. R.; Martens, H. In *Handbook of Near-Infrared Analysis*; Burns, D. A., Ciurczak, E. W., Eds.; Dekker: New York, 2001; pp 185−207.

(12) Thomas, L. C.; Greenstreet, J. E. S. The identification of microorganisms by infrared spectrophotometry. *Spectrochim. Acta* **1954**, *6*, 302–319.

(13) Riddle, J. W.; Kabler, P. W.; Kenner, B. A.; Bordner, R. H.; Rockwood, S. W.; Stevenson, H. J. R. Bacterial identification by infrared spectrometry. *J. Bacteriol.* **1956**, *72*, 593–603.

(14) Goulden, J. D. S.; Sharpe, M. E. The infra-red absorption spectra of lactobacilli. *J. Gen. Microbiol.* **1958**, *19*, 76–86.

(15) Norris, K. P. Infra-red spectroscopy and its application to microbiology. *J. Hyg.* **1959**, *57*, 326–345.

(16) ScopesA. W. The infrared spectra of some acetic acid bacteria. *J. Gen. Microbiol.* **1962**, *28*, 69–79.

(17) Naumann, D.; Helm, D.; Labischinski, H.; Giesbrecht, P. In *Modern Techniques for Rapid Microbiological Analysis*; Nelson, W. H., Ed.; VCH: New York, 1991; p 43.

(18) Ellis, D. I.; Broadhurst, D.; Bell, D. B.; Rowland, J. J.; Goodacre, R. Rapid and quantitative detection of the microbial spoilage of meat by fourier transform infrared spectroscopy and machine learning. *Appl. Environ. Microbiol.* **2002**, *68* (6), 2822–2828.

(19) Al-Qadiri, H. M.; Al-Holy, M. A.; Lin, M.; Alami, N. I.; Cavinato, A. G.; Rasco, B. A. Rapid detection and identification of *Pseudomonas aeruginosa* and *Escherichia coli* as pure and mixed cultures in bottled drinking water using fourier transform infrared spectroscopy and multivariate analysis. *J. Agric. Food Chem.* **2006**, *54*, 5749–5754.

(20) Rodriguez-Saona, L. E.; Khambaty, F. M.; Fry, F. S.; Calvey, E. M. Rapid detection and identification of bacterial strains by Fourier transform near-infrared spectroscopy. *J. Agric. Food Chem.* **2001**, *49*, 574–579.

(21) Dubois, J.; Lewis, E. N.; Fry, F. S., Jr.; Calvey, E. M. Bacterial identification by near-infrared imaging of food specific-cards. *Food Microbiol.* **2005**, *22*, 577–583.

(22) Lin, M.; Al-Holy, M.; Mousavi-Hesary, M.; Al-Qadiri, H.; Cavinato, A. G.; Rasco, B. A. Rapid and quantitative detection of the microbial spoilage in chicken meat by diffuse reflectance spectroscopy (600–1100 nm). *Lett. Appl. Microbiol.* **2004**, *39*, 148–155.

(23) Rodriguez-Saona, L. E.; Khambaty, F. M.; Fry, S. F.; Dubois, J.; Calvey, E. M. Detection and identification of bacteria in a juice matrix with Fourier transform-near infrared spectroscopy and multivariate analysis. *J. Food Prot.* **2004**, *67* (11), 2555–2559.

(24) Suthiluk, P.; Saranwong, S.; Kawano, S.; Numthuan, S.; Satake, T. Possibility of using near infrared spectroscopy for evaluation of bacterial contamination in shredded cabbage. *Int. J. Food Sci. Technol.* **2008**, *43*, 160–165.

(25) Savitzky, A.; Golay, M. J. E. Smoothing and differentiation of data by simplified least squares procedures. *Anal. Chem.* **1964**, *36*, 1627–1639.

(26) Williams, P. C.; Norris, K. H. *Near-Infrared Technology in the Agricultural and Food Industry*; American Association of Cereal Chemists: St. Paul, MN, 1987.

(27) Heller, D. N.; Cotter, R. J.; Fenselau, C.; Uy, O. M. Profiling of bacteria by fast-atom-bombardment-mass spectrometry. *Anal. Chem.* **1987**, *59*, 2806–2809.

(28) Cole, M. J.; Enke, C. G. Direct determination of phospholipid structures in microorganisms by fast atom bombardment triple quadrupole mass spectrometry. *Anal. Chem.* **1991**, *63*, 1032–1038.

(29) Harrington, P. B.; Street, T. E.; Voorhees, K. J.; Brozoo, F. R.; Odom, R. W. A rule-building expert system for classification of mass spectra. *Anal. Chem.* **1989**, *61*, 715–719.

(30) Marr, A. G.; Ingraham, J. L. Effect of temperature on the composition of fatty acids in *Escherischia coli*. *J. Bacteriol.* **1962**, *84* (6), 1260–1267.

Received for review November 21, 2007. Revised manuscript received February 28, 2008. Accepted March 3, 2008.

JF073407X